Molecular Therapy
Nucleic Acids
Original Article

Single-cell profiling of mouse and primate ovaries identifies high levels of *EGFR* for stromal cells in ovarian aging

Ye Wei,[1,7] Ruidi Yu,[1,7] Sheng Cheng,[1,4,7] Ping Zhou,[3,7] Shaomei Mo,[2,5] Chao He,[1] Chang Deng,[1] Peng Wu,[6] He Liu,[2] and Canhui Cao[1,2,3]

[1]Department of Gynecology and Obstetrics, Key Laboratory of the Ministry of Education, Tongji Hospital, Tongji Medical College, Huazhong University of Science and Technology, Wuhan 430030, China; [2]Department of Gastrointestinal Surgery, Reproductive Research Institute, Peking University Shenzhen Hospital, Guangdong 518036, China; [3]Center for Reproductive Medicine, Department of Obstetrics and Gynecology, Peking University Third Hospital, Beijing 100191, China; [4]National Key Laboratory of Crop Genetic Improvement, Huazhong Agricultural University, Wuhan 430070, China; [5]The Fifth Clinical College, Anhui Medical University, Hefei 230000, China; [6]Department of Gynecology and Obstetrics, Union Hospital, Tongji Medical College, Huazhong University of Science and Technology, Wuhan 430030, China

Increased ovarian fibrosis and an expanded stromal cell compartment are the main characteristics of aging ovaries. However, the molecular mechanisms and the key factor of stromal cells underlying ovarian aging remain unclear. Here, we explored single-cell transcriptomic data of ovaries from the adult mouse (4,363 cells), young (1,122 cells), and aged (1,479 cells) non-human primates (NHPs) to identify expression patterns of stromal cells between young and old ovaries. An increased number of stromal cells (p = 0.0386) was observed in aged ovaries of NHPs, with enrichment processes related to the collagen-containing extracellular matrix. In addition, differentially expressed genes of stromal cells between young and old ovaries were regulated by ESR1 (p = 7.94E-08) and AR (p = 1.99E-05). Among them, *EGFR* was identified as the common target and was highly expressed (p = 7.69E-39) in old ovaries. In human ovaries, the correlated genes of *EGFR* were associated with the process of the cell-substrate junction. Silencing of *EGFR* in human ovarian stromal cells led to the reduction of cell-substrate junction via regulating phosphorylation modification of the AKT-mTOR signaling pathway and stromal cell marker genes. Overall, we identified high levels of *EGFR* for stromal cells in ovarian aging, which provides insight into the cell type-specific molecular mechanisms underlying ovarian aging at single-cell resolution.

INTRODUCTION

The ovary is an indispensable female reproductive organ for female reproductive development, fertility maintenance, and endocrine homeostasis, which produces oocytes and steroid hormones.[1,2] The structure of the ovary is complex, composed of multiple heterogeneous cell types at different stages, including follicles, oocytes, and surrounding granulosa cells and/or membranous cells.[3] The aging of the female reproductive system is a common fertility problem, because women's childbearing age is gradually delayed, resulting in a higher incidence of infertility, miscarriage, and birth defects.[4] In addition to its indispensable function in female fertility, ovaries also play a regulatory role in health.[5] Other diseases, such as ovarian cancer, type 2 diabetes, breast cancer, cardiovascular disease, osteoporosis, and fractures could be also related to ovarian aging.[6] An in-depth understanding of the mechanisms that drive ovarian aging is essential.

Although functional decline along with ovarian aging has been recognized, the molecular changes are not well defined. There is an urgent need to understand the physiological and cellular mechanisms of female reproductive system aging.[7] With age, the number and quality of oocytes decrease, the number of follicles decreases, and the number and function of granulosa cells are abnormal.[8] In addition, increased inflammation, accumulation of reactive oxygen species, and aging-related anatomical and physiological changes, including altered extracellular matrix, changes in medulla and cortex volume, and extensive tissue fibrosis, are closely associated with ovarian aging.[9,10]

Fibrosis is characterized by the accumulation of collagen I and III and organ dysfunction, which is a common hallmark of several aging organs.[11] Like other organs, the ovaries of mammals become increasingly fibrotic with age, which is conserved between mice and

Received 28 July 2022; accepted 22 November 2022;
https://doi.org/10.1016/j.omtn.2022.11.020.

[7]These authors contributed equally

Correspondence: Peng Wu, Department of Gynecology and Obstetrics, Union Hospital, Tongji Medical College, Huazhong University of Science and Technology, Wuhan 430030, China
E-mail: pengwu8626@tjh.tjmu.edu.cn
Correspondence: He Liu, Department of Gastrointestinal Surgery, Reproductive Research Institute, Peking University Shenzhen Hospital, Guangdong 518036, China.
E-mail: liuhe199024@163.com
Correspondence: Canhui Cao, Department of Gynecology and Obstetrics, Key Laboratory of the Ministry of Education, Tongji Hospital, Tongji Medical College, Huazhong University of Science and Technology, Wuhan, Hubei 430030, China.
E-mail: canhuicao@foxmail.com

humans.[9] Fibrosis in aged ovaries was related to increased ovarian stromal cells, which could affect the shape of follicles.[8] Ovarian stroma is composed of a population of cells commonly described as stromal cells,[12] including the populations of fibroblast-like cells, spindle-shaped cells, or interstitial cells.[13] In general, extracellular matrix (ECM) was produced by stromal fibroblast-like cells, such as collagen I, III, IV, and VI.[14] Theca interstitial cells showed a fibroblast-like appearance when primary cultured *in vitro*,[15] and interstitial cells are responsible for the features of steroid production in the human fetal gonads.[16] However, the key factor of stromal cells in ovarian aging remained to be determined.

Because of the heterogeneous population of the ovary, conventional RNA sequencing (RNA-seq) has difficulties in identifying cell type-specific changes in young and old ovaries.[17] In addition, ethical restrictions and the limited access to obtain disease-free human young ovaries make it difficult to study ovarian aging. An appropriate model could help scientists to identify the risk factors and molecular mechanisms underlying ovarian aging.[18] Fortunately, with the development of single-cell RNA sequencing technology, it is possible to analyze expression patterns of heterogeneous tissues at the single-cell level.[2] Furthermore, because non-human primates (NHPs) share similar genomic and physiological characteristics with humans, young and old ovaries of NHPs were generated as a model for studying ovarian aging *in vivo*.[19] With advances in the single-cell RNA sequencing of primate ovaries, the single-cell transcriptomic atlas of young and old ovaries of NHPs was used to study the molecular mechanisms underlying ovarian aging.[20] These single-cell RNA-seq data were generated using certified methods with high quality in gene expression and were published in top academic journals,[2,20] which would effectively explore the cell type-specific molecular mechanisms of stroma cells underlying ovarian aging.

In this study, we used public single-cell transcriptomic data of ovaries from the adult mouse (4,363 cells), young (1,122 cells), and aged (1,479 cells) non-human primates to identify expression patterns and specific markers of stromal cells in young and old ovaries. Tans-omics data of chromatin immunoprecipitation sequencing (ChIP-seq), RNA-seq, and proteomics were analyzed to demonstrate the roles of *EGFR* in ovarian stromal cells. Primary cultured stromal cells of the ovary were used to verify the biological role of *EGFR* in ovarian stromal cells, which provides insight into the cell type-specific molecular mechanisms underlying ovarian aging at single-cell resolution.

RESULTS

Single-cell transcriptome analysis of the adult mouse ovary

Because the ovary is a complex organ that consists of numerous cell types, including oocytes, luteal cells, stromal cells, smooth muscle cells, immune cells, and others,[2] understanding the gene expression patterns and identifying specific marker genes of each cell type is necessary. We analyzed single-cell transcriptomic data of the adult mouse ovary from the mouse cell atlas[20]; 4,363 cells were clustered into 14 sub-types according to the gene expression of each cell (Figure 1A). There were 484 stromal cells, accounting for 11% of all ovary cells (Figure S1A). By analyzing marker genes of stromal cells, we identified 280 marker genes of stromal cells (Table S1) and found that the expression markers were enriched in the processes related to an extracellular matrix organization, focal adhesion, smooth muscle contraction, and so on (Figure 1B; Figure S1B). In transcription factor (TF) analysis, these markers were mainly regulated by RELA, SP1, NFKB1, and ESR1 (Figure S1C). The top marker genes of stromal cells were shown in Figure 1C, such as *Acta2*, and *Bgn*, with specific expression in the C4 cluster (Figure 1C). In addition, the specific gene expression patterns were validated by immunofluorescence in adult mouse ovaries (Figure 1D).

Single-cell transcriptome analysis of primate ovaries identified the increased stromal cells in ovarian aging

To identify the characteristics of young and old ovaries, we explored the single-cell transcriptomic data of ovaries from young (n = 4, 4–5 years old) and old (n = 4, 18–20 years old) non-human primates.[2] In total, 2,601 cells from primate ovaries were clustered into 8 clusters according to the gene expression of each cell (Figure 2A). There were 1,203 stromal cells, accounting for 46% of all ovary cells (Figure S2A). When analyzing the specific marker genes with the mouse stromal cells, we found 60 overlapped markers between them (Figure 2B; Table S2), which were significantly enriched in the disease of fibrosis (Figure 2C). Importantly, we found that stromal cells were increased in old ovaries ($p = 0.0386$) compared with young ovaries (Figure 2D). Although smooth muscle cells were also the mesenchymal components (9%) in primate ovaries, there were no statistical differences in the smooth muscle cell cluster between the young and old ovaries (Figure 2E). By analyzing differentially expressed genes (DEGs) of stromal cells between young and old ovaries, 63 DEGs were identified (Table S3), with the enrichment in the processes related to extracellular matrix binding, collagen binding, and collagen-containing extracellular matrix, and so on (Figures 2F and S2B). In transcription factor analysis, these DEGs were enriched in ESR1 and AR (Figure 2G). Moreover, the expanded ovarian fibrosis was validated by Masson's staining in ovaries of young and old ovaries (Figures 2H and 2I).

Integrative analysis identified *EGFR* was highly expressed in old ovaries

AR and ESR1 are steroid-activated TFs that play key roles in cellular biology.[21] To further analyze the gene expression patterns of stromal cells between young and old ovaries of NHPs, we compared the DEGs of stromal cells with targets of ESR1 and AR, and we found that there were 3 overlapped genes (*EGFR*, *BTG2*, and *MYC*) among them (Figure 3A). In single-cell transcriptomic data of young and old ovaries, *EGFR* ($p = 7.69E-39$), *BTG2* ($p = 7.30E-09$), and *MYC* ($p = 3.03E-11$) were highly expressed in stromal cells of old ovaries (Figure 3B).

Next, we explored the correlation between ESR1 or AR and target genes in RNA-seq data of human ovaries (n = 180) and found that the expression of *EGFR* showed positive correlation with that of *ESR1* ($p = 1.00E-07$, $R = 0.53$) and *AR* ($p = 0.0087$, $R = 0.28$) in human

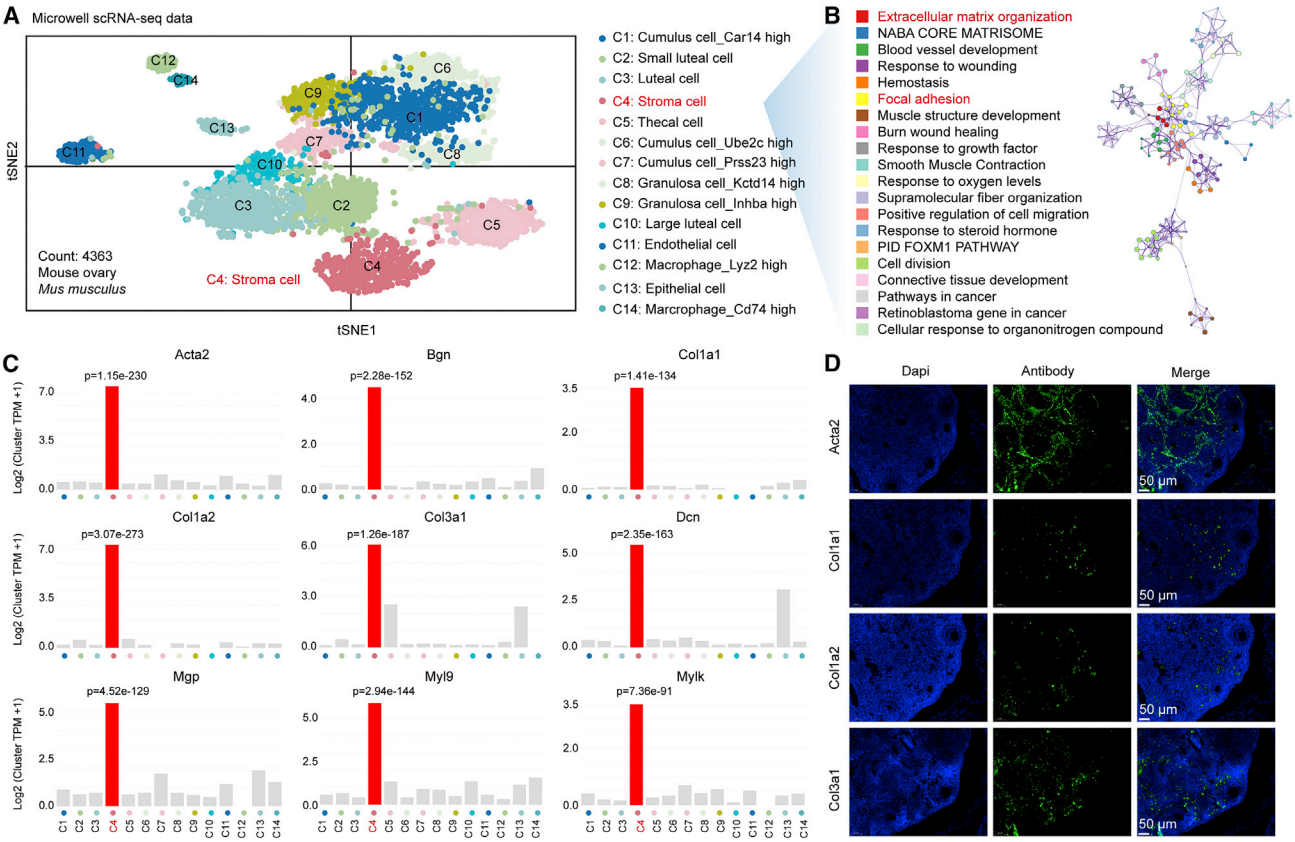

Figure 1. Single-cell transcriptome analysis of the adult mouse ovary

(A) t-SNE map of single-cell transcriptomic data of the adult mouse ovary. Cells were clustered into 14 types with different colors, and each dot represents a cell. (B) Enrichment and pathway analysis of specific markers of cluster 4 (stromal cells). (C) Gene expression level of each cell cluster in the adult mouse ovary, with p value in C4 cluster. The y axis represents the $\log_2$ (cluster mean expression TPM + 1). (D) Immunofluorescence staining of *Acta2*, *Col1a1*, *Col1a2*, and *Col3a1* in the mouse ovary.

ovaries (Figures 3C and 3D). In transcription factors analysis from Toolkit,[22] AR and ESR1 showed a high regulatory potential score in the *EGFR* gene (Figure 3E), and the high scores of AR and ESR1 were not observed in *BTG2* and *MYC* (Figures S3A and S3B). Furthermore, we downloaded and analyzed ChIP-seq data of AR and ESR1 from the public datasets and found that peaks of AR and ESR1 were enriched in the same region of the *EGFR* gene (Figure 3F). The ChIP-seq peak enrichment region of *EGFR* was found to be a promoter of the *EGFR* gene via analyzing the *cis*-regulatory elements from all cell types (Figure 3G). These results indicated that *EGFR* was highly expressed in old ovaries, which was associated with the expression of AR and ESR1 in ovaries.

High expression of *EGFR* in stromal cells was associated with the cell-substrate junction process in human ovaries

In single-cell transcriptomic data of the mouse ovary, *Egfr* showed a higher expression level in stroma cells (cluster 4, Figure 4A). According to previous studies of The Jackson Laboratory, the mouse age range of 3–6 months is defined as a young age that is correlated with 20–30 years of age in humans, and the mouse age range of 18–24 months is defined as an old age that is correlated with 56–69 years of age in humans. Therefore, we performed immunofluorescence staining of young (4 months) and old (20 months) mouse ovaries, and we found that *Egfr*, *Acta2*, *Ar*, and *Esr1* were highly expressed in old mouse ovaries, with the reduction of the primordial follicle, primary follicle, secondary follicle, and antral phase follicle in old mouse (Figures 4B, 4C, and S4A).

To identify the molecular roles of *EGFR* in human ovaries, we explored proteomics data of human ovaries (n = 8) from GTEx Portal and performed a correlation analysis of *EGFR* in human ovaries and compared them with the marker genes of primate ovarian stromal cells (Figures 4D–4G). The positively correlated genes of *EGFR* in stromal cells were associated with the processes related to the cell-substrate junction, cell adhesion molecule binding, cadherin binding, cell-substrate adherens junction, focal adhesion, and so on (Figure 4E). Protein-protein interaction networks of the positively correlated genes of *EGFR* in stromal cells were associated with functional enrichment of mRNA splicing, cell cycle, and so on (Figures S4B and S4C). Although *CAMK2N2* was identified as an *EGFR* negatively correlated

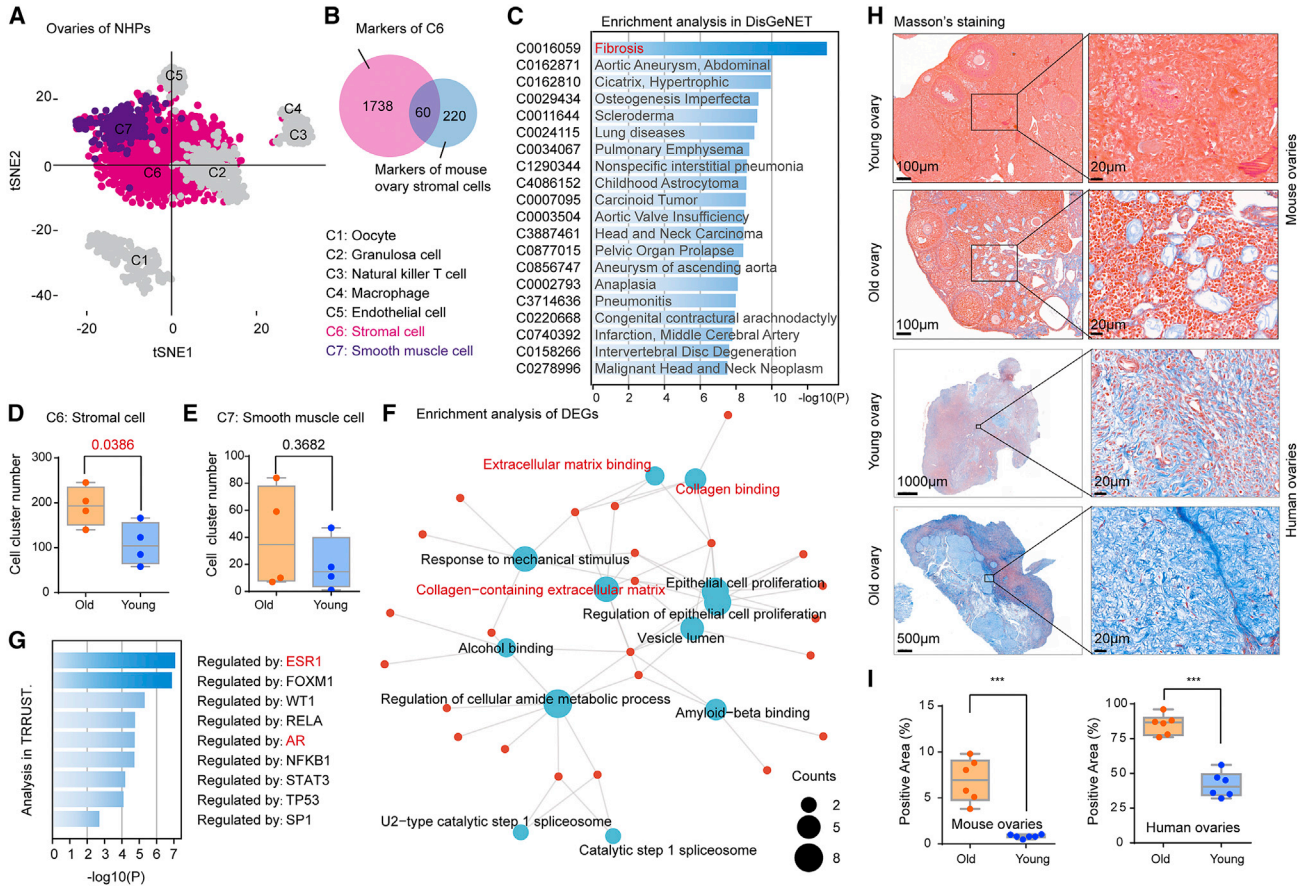

Figure 2. Single-cell transcriptome analysis of primate ovaries identified the increased stromal cells in ovarian aging

(A) t-SNE map of single-cell transcriptomic data of non-human primate ovaries. (B) Venn diagram of stromal cell markers between primate ovaries and the adult ovary, with 60 overlapped genes. (C) Enrichment analysis of 60 overlapped genes in DisGeNET. (D) Cell number of stromal cells in old and young primate ovaries. (E) Cell number of smooth muscle cells in old and young primate ovaries. (F) Enrichment and pathway analysis of DEGs of stromal cells between young and old primate ovaries. (G) Enrichment analysis of DEGs in TRRUST. (H and I) Masson's trichrome staining (H) and statistical analysis (I) between young and old ovaries. Data are presented as mean ± SD. *$p < 0.05$, **$p < 0.01$, and ***$p < 0.001$.

gene, it was not a marker gene of stroma cells in NHP and mouse ovaries (Figure 4F). The negatively correlated genes of *EGFR* in stromal cells were associated with the processes related to the transcription factor complex and RNA polymerase II transcription factor complex (Figure 4G).

Silencing of *EGFR* inhibited cell-substrate junction and promoted cellular senescence in ovarian stromal cells via the AKT-mTOR signaling pathway

To demonstrate the roles of *EGFR* in ovarian stromal cells, we isolated primary cultured stromal cells from the human ovary and validated the markers of stromal cells (Figure 5A). We then performed an ECM cell adhesion assay of ovarian stromal cells by interfering with the expression of *EGFR* (si-*EGFR*) compared with normal control (si-NC), and we found the reduction of ovarian stromal cells after interfering with the expression of *EGFR* (Figures 5B and 5C). In addition, the increased cellular senescence of ovarian stromal cells was observed in the si-*EGFR* groups (Figures 5D and 5E).

Previous studies have shown that PI3K/AKT signaling is a key downstream mechanism of *EGFR* in an aging model.[23,24] Therefore, we performed an ECM cell adhesion assay and cultured them for 24 h before immunofluorescence staining. After validating the expression of EGFR and ACTA2, we found that the expression of p-AKT and p-mTOR was inhibited after si-*EGFR* in stromal cells (Figure 5F). In addition, the phosphorylation modification of the AKT-mTOR signaling pathway was validated by western blot, and the expression of stromal cell markers (ACTA2, COL1A1, COL1A2, COL3A1) were down-regulated after si-*EGFR* (Figure 5G). Taken together, our results showed that silencing of *EGFR* inhibits cell-substrate junction and promoted cellular senescence via the AKT-mTOR signaling pathway.

RNA-seq data demonstrated that silencing of *EGFR* was associated with aging and cell-cell adhesion in ovarian stromal cells

To validate the role of *EGFR* in ovarian stromal cells, we performed RNA-seq analysis of primary cultured ovarian stromal cells by

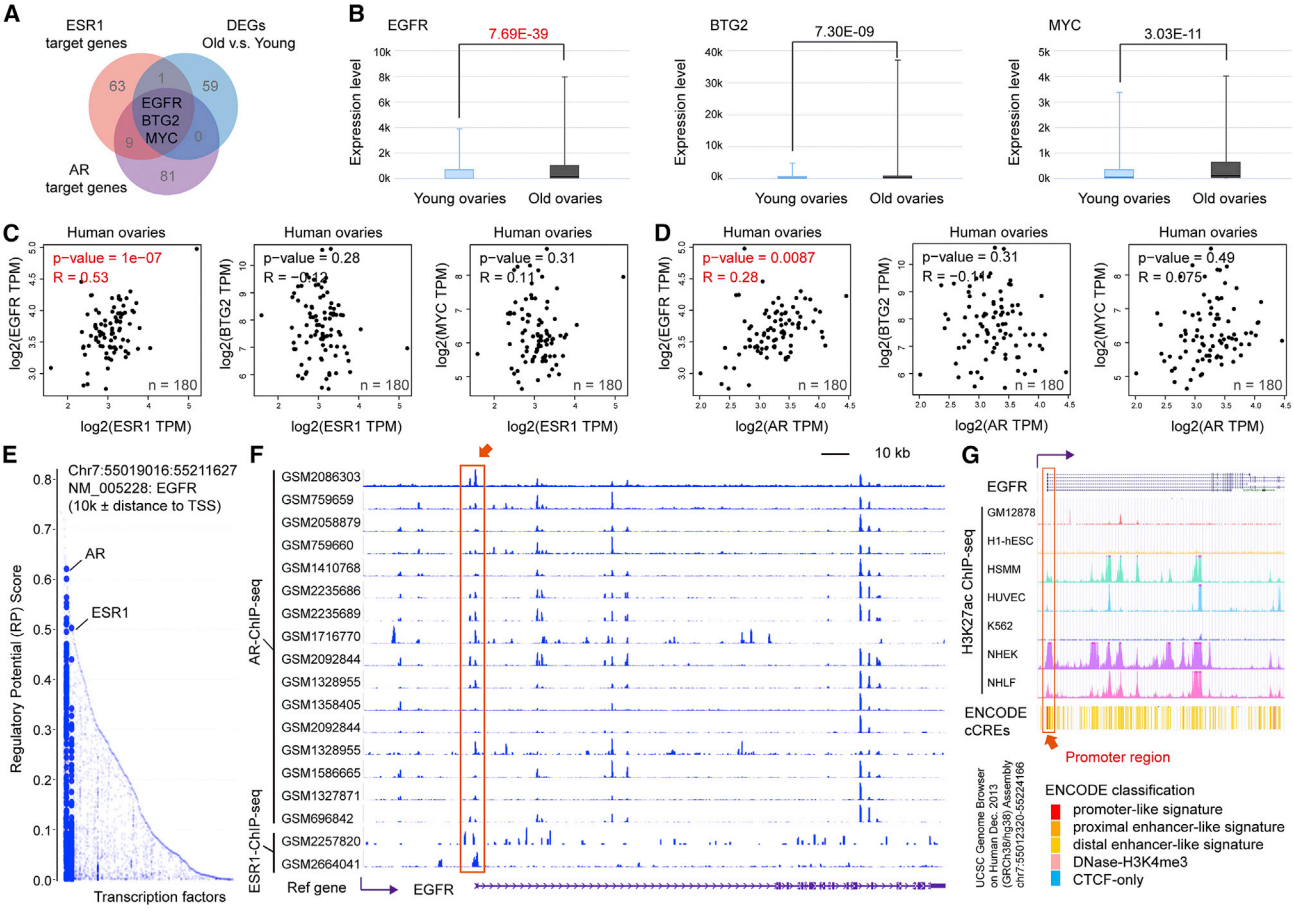

Figure 3. Integrative analysis identified that *EGFR* was highly expressed in old ovaries

(A) Venn diagram of DEGs of stromal cells between young and old primate ovaries, targets genes of AR and ESR1, with 3 overlapped genes. (B) Gene expression levels of *EGFR*, *BTG2*, and *MYC* in stromal cells of young and old primate ovaries. (C and D) Correlation analysis of target genes (*EGFR*, *BTG2*, and *MYC*) with ESR1 (C) and AR (D) in human ovaries. (E) The regulatory potential score of transcription factors in the *EGFR* genes. (F) ChIP-seq peaks of ESR1 and AR in the *EGFR* gene. (G) *cis*-Regulatory elements analysis of *EGFR* gene region from UCSC Genome Browser.

si-*EGFR* and si-NC. By interfering with *EGFR* of ovarian stromal cells, 500 DEGs were significantly identified between the two groups (Table S4). Among the DEGs, *EGFR* was significantly inhibited in the si-*EGFR* group (Figure 6A). By analyzing the enriched pathway and process of DEGs form Metascape, signaling by GPCR (R-HSA-372790), cell activation (GO:0001775), positive regulation of cell migration (GO:0030335), aging (GO:0007568), and cell-cell adhesion (GO:0098609) were enriched (Figure 6B).

We then explored the RNA-seq data of NIH3T3 (a stromal cell line) with *Egfr* mutants (Del1, L858R, L861Q),[25] and we found that PI3K-AKT signaling pathway was enriched after *Egfr* mutant's transfection compared with wild-type and empty vector (Figures S5A–S5C). In addition, extracellular matrix organization, degradation of the ECM, and ECM regulators were enriched in gene set enrichment analysis (GSEA) (Figure 6C). In addition, by analyzing single-cell RNA-seq data from young and old ovary tissue and RNA-seq data of si-*EGFR*. *EGFR* was observed in si-*EGFR* down-regulation group and the old ovary up-regulation group (Figures S5D–S5F). The overlapped genes were associated positive regulation of biological process (GO:0048518), biological regulation (GO:0065007), and cellular process (GO:0009987) (Figure S5E). Importantly, the genes related to aging (GO:0007568) and cell-cell adhesion (GO:0098609) were analyzed, which was mentioned to be related ovarian aging in the previous analysis (Figures 6D and 6E). Moreover, genes related to aging (GO:0007568) and cell-cell adhesion (GO:0098609) were validated to be down-regulation after interfering with *EGFR* in ovarian stromal cells (Table S5; Figures 6F and 6G).

DISCUSSION

The human ovary, a female reproductive organ, exhibits dysfunction of early-onset aging in the human body after only the age of 30 years.[4] In aged ovaries, increased ovarian fibrosis and expanded stromal cell compartments were known as the main characteristics.[26] Herein, we

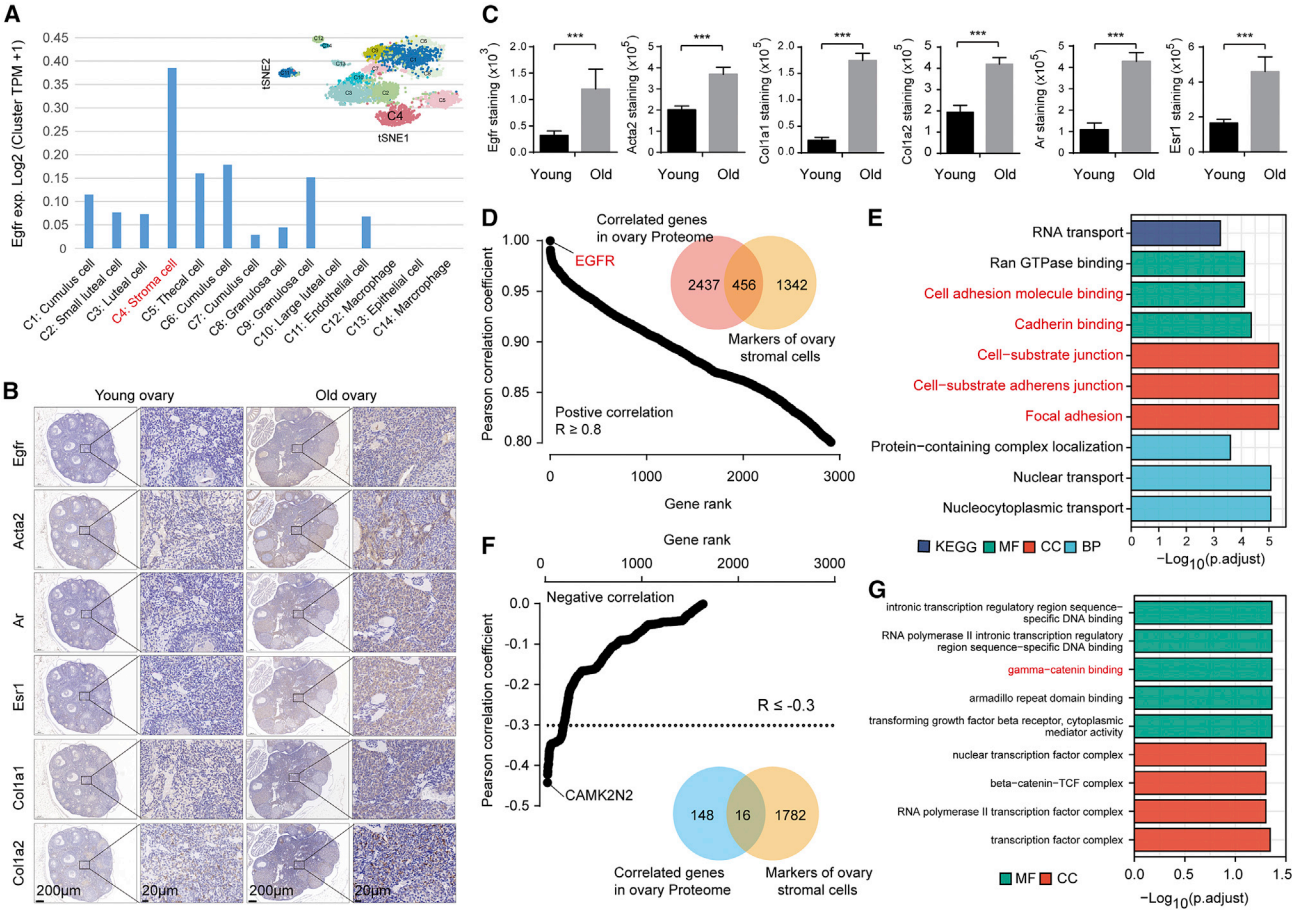

Figure 4. High expression of *EGFR* in stromal cells was associated with the cell-substrate junction process in human ovaries

(A) *Egfr* expression level of each cell cluster in the adult mouse ovary. Y axis represents the $\log_2$ (cluster mean expression TPM + 1). (B and C) IHC staining (B) and statistical analysis (C) of Egfr, Acta2, Ar, Esr1, Col1a1, and Col1a2 in young and old mouse ovaries. Data are presented as mean ± SD. p value was calculated using Student's t test. (D) Positively correlated genes of *EGFR* in the proteomics data of human ovaries and the Venn diagram of positively correlated genes and marker genes of stromal cells in primate ovaries. (E) Enrichment and pathway analysis of DEGs of 456 overlapped genes. (F) Negatively correlated genes of *EGFR* in the proteomics data of human ovaries and the Venn diagram of negatively correlated genes and marker genes of stromal cells in primate ovaries. (G) Enrichment and pathway analysis of DEGs of 16 overlapped genes. *p < 0.05, **p < 0.01, ***p < 0.001.

explored single-cell transcriptomic data of primate and mouse ovaries to demonstrate the gene expression patterns of stromal cells in young and old ovaries and identified *EGFR* as a basis for stromal cells in ovarian aging. The analysis of aging-associated gene expression patterns of primate ovaries revealed cell type-specific molecular mechanisms of stroma cells underlying ovarian aging at single-cell resolution.

Ovarian aging is associated with the function of various cellular biology, such as mitochondrial dysfunction, epigenetic dysregulations, and/or metabolic disorders.[27] Previous studies have used *DCN*, *LUM*, *PDGFRA*, *COL1A1*, *COL6A1*, *STAR*, *TCF21*, *COL1A2*, and/or *CYP17A1* to characterize the markers of ovarian stromal cells,[28] which were also identified in our single-cell transcriptomic results from the mouse adult ovary. Organ fibrosis is reputed as a hallmark of organ aging and often leads to altered structure and dysfunction.[29] In our results, common marker genes of stromal cells in ovaries of the adult mouse and NHPs were associated with disease in fibrosis. In addition, ovarian aging is reported to be correlated with increased ovarian fibrosis expanded by changes in ovarian stromal composition, namely, stromal cells and ECM,[7] which was consistent with the results that stromal cells were increased in old ovaries of NHPs than that of young NHPs.

Increasing evidence showed the correlation between *EGFR* and aging or aging-related diseases.[30–36] However, the roles of *EGFR* in ovarian aging remain unclear, especially in stromal cells underly ovarian aging. Nautiyal et al.[30] revealed that aging of the gastrointestinal tract are associated with the increased tyrosine-phosphorylated EGFR, and inhibiting *EGFR* reversed the age-related increment of *CD166*, *ALDH-1*, and *miR-21*. Earlier studies also found that the rise of age-related factors in colonic cancer stem-like cells was correlated

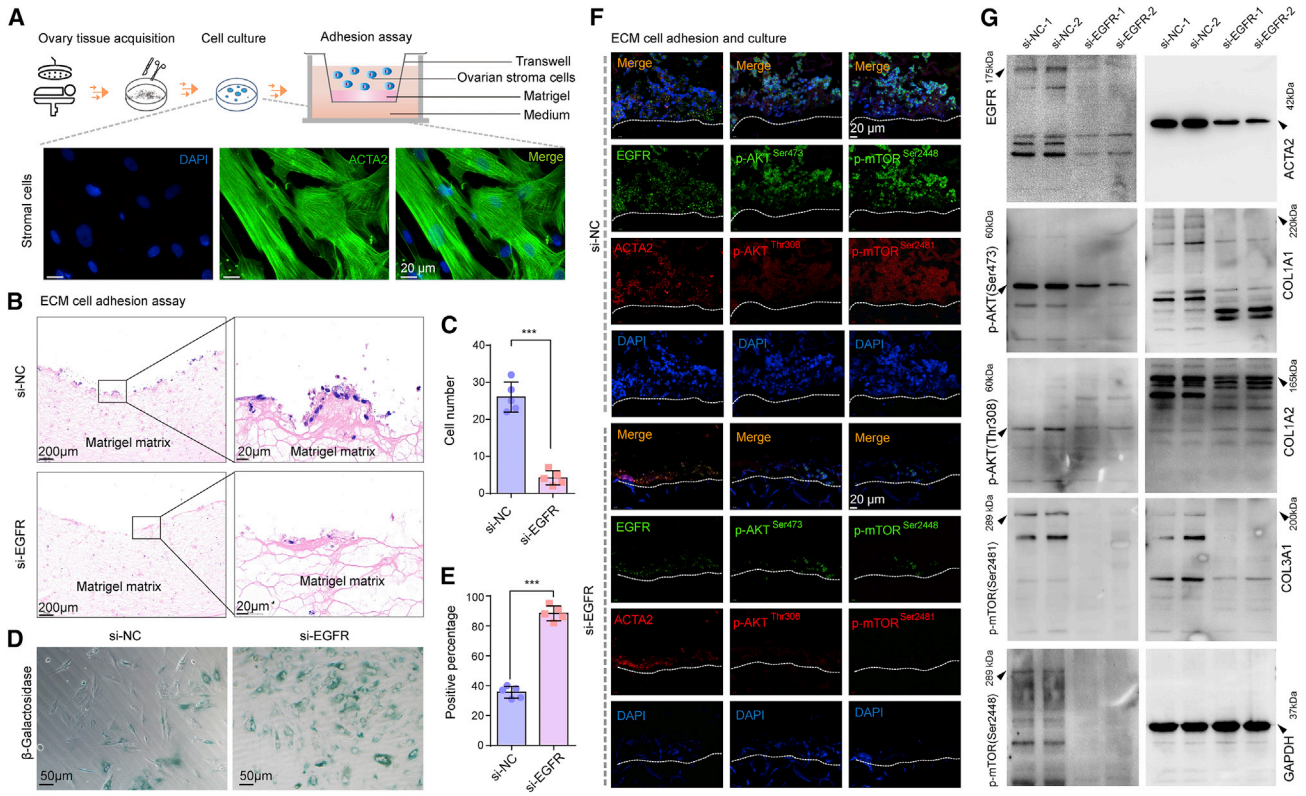

Figure 5. Silencing of *EGFR* inhibited cell-substrate junction and promoted cellular senescence in ovarian stromal cells via AKT-mTOR signaling pathway

(A) The schematic diagram of the stromal cell isolation and ECM cell adhesion assay; validation of ACTA2 immunofluorescence is displayed at the bottom. (B and C) H&E staining (B) and statistical result (C) of ECM cell adhesion assay between the si-*EGFR* and si-NC group. (D and e) Cellular senescence staining (D) and statistical result (E) of ovarian stromal cells between the si-*EGFR* and si-NC groups. Data are presented as mean ± SD. p value was calculated using Student's t test. (F) Stromal cells were performed by ECM cell adhesion assay and cultured for 24 h. Immunofluorescence was conducted to compare the expression of the AKT-mTOR signaling pathway between the si-*EGFR* and si-NC groups. (G) Western blot of stromal cells between the si-*EGFR* and si-NC groups. *p < 0.05, **p < 0.01, and ***p < 0.001.

with the activation of *EGFR*.[31,32] Siddiqui et al.[33] systematically reviewed the multidimensional roles of *EGFR* in the aging of neurometabolic processes. The roles of *EGFR* in cellular senescence are identified to be bidirectional effects. In ovarian stromal cells, we found that silencing of *EGFR* induced the reduction of the cell-substrate junction and the increment of cellular senescence *in vitro*. These were consistent with the findings that down-regulation of *EGFR* mediates cellular senescence by activation of p53 in some types of cancer cells.[34] However, in IMR90 cells, activation of *EGFR* induced cellular senescence via increasing senescence-associated factors.[35] In addition, inhibiting *EGFR* signaling by gefitinib promoted cellular senescence of osteoprogenitors and decreased bone formation in middle-aged mouse models.[36]

Of note, ovarian stromal cells can produce steroid hormone and express hormone receptors.[13] Estrogen receptors alpha (ESR1) and beta (ESR2) have been identified in the cytoplasm and nucleus of interstitial cells in the bovine ovary.[37] Progesterone receptor alpha (PRα) has been documented in stromal cells and interstitial cells in the rabbit ovary.[38] In addition, AR was observed in stroma cells from fetal gonad in the sheep ovary.[39] Moreover, steroidogenic enzymes (*STAR* and *CYP11A1*) have been identified in the stromal cell cluster in single-cell RNA-seq studies.[2,28] Women at an advanced age are often marked by ovarian fibrosis in the stroma, increased androgen production in stromal cells, and increased levels of basal LH,[40–42] with the evidence that the stromal cells of the postmenopausal ovary are the important source of androgen.[43] In our results, DEGs of stromal cells between young and old ovaries were regulated by ESR1 and AR in transcription factor analysis, which might explain the expression changes of stromal cells underlying ovarian aging regulated by the changes of steroid hormone and/or hormone receptors.

The mouse model has long been used to gain insights into gene function in human disease development due to the conversed events between human and mouse tissues.[44,45] However, researchers found that mice with the same genetic changes and/or pathogenic mutations do not display the human phenotype.[46–48] These functional differences may be the differences in gene expression patterns between mouse and human tissues.[48] In our study, gene expression patterns of ovarian stromal cells between mice and NHPs showed differences in single-cell resolution. Most of the maker genes in NHP ovarian stromal cells were not observed in mouse ovarian stromal cells.

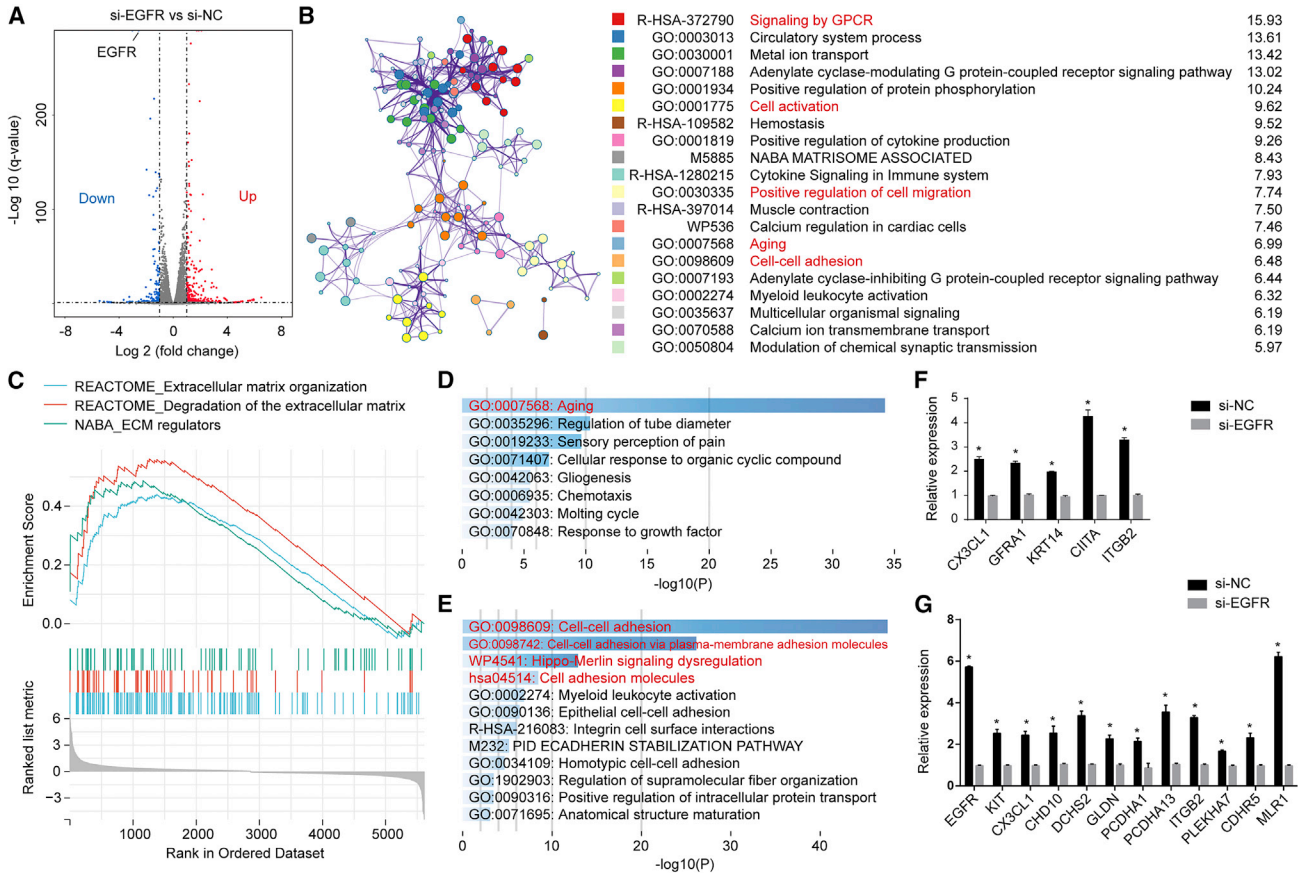

Figure 6. RNA-seq data demonstrated that silencing of *EGFR* was associated with aging and cell-cell adhesion in ovarian stromal cells

(A) Volcano plot of DEGs between si-*EGFR* and si-NC in ovarian stromal cells. *EGFR* gene is indicated. (B) Enrichment and pathway analysis of DEGs between si-*EGFR* and si-NC in ovarian stromal cells. (C) GSEA of DEGs between si-*EGFR* and si-NC in ovarian stromal cells. (D and E) Enrichment and pathway analysis of aging-related genes (GO:0007568) (D) and cell-cell adhesion related genes (GO:0001775) (E). Real-time PCR of aging-related genes (F) and cell-cell adhesion related genes (G) between si-*EGFR* and si-NC in ovarian stromal cells (mean±SD). p value was calculated using Student's t test. *p < 0.05, **p < 0.01, and ***p < 0.001.

The present findings were based on the descriptive analysis of single-cell transcriptome analysis of ovaries, identifying the potential genes of stromal cells in multi-regulatory networks. Given that ovary is a complex organ with multi-cell types, it is important to understand the mechanisms of *EGFR* in the stroma cell population underlying ovarian aging *in vivo*. In addition, the molecular roles of *EGFR* in ovarian aging may differ from the primary cultured ovarian stromal cells, which means that the *in vivo* changes of the *EGFR* activation may differ from the cellular responses of *EGFR* silencing-mediated changes. The best way to know the role of *EGFR* for stromal cells in ovarian aging is to conduct an *in vivo* mouse model, such as an ovarian stromal cell-Egfr-knockout mouse model ($Egfr^{flox+/-,\ Cyp17a1\text{-}Cre}$). Furthermore, subsequent studies should be performed to identify which of these mechanisms is responsible for the expansion of the stromal cell population in ovarian aging.

In conclusion, this study explored the expression patterns and differential expression of stroma cells in the mouse and young and old non-human primate ovaries at single-cell resolution. The expression patterns and differential changes were enriched in the process related to fibrosis and extracellular matrix binding, with the *EGFR* high expression in the old ovaries. ChIP-seq analysis demonstrated that peaks of AR- and ESR1-ChIP-seq were enriched in the promoter region of target *EGFR*, which was associated with a high expression status of *EGFR*. In aged ovaries, increased expression of *EGFR* was associated with cell-substrate junction and was reversed by silencing of *EGFR*. These results from our study suggest that *EGFR* may be a promising target for ovarian aging.

MATERIALS AND METHODS

Data acquisition and single-cell transcriptomic analysis

Single-cell RNA-seq data of the mouse ovary were downloaded from GSE108097,[20] it was generated by the Microwell-Seq protocol. In total, 4,363 cells of the adult ovary were processed by Seurat for dimension reduction (t-distributed stochastic neighbor embedding [t-SNE]), cell clustering (14 cell clusters), and differential gene expression analysis. Single-cell RNA-seq data of young (n = 4) and

aged (n = 4) non-human primates were downloaded from GSE1 30664, which were generated using the STRT-seq protocol.[2] In total, 2,601 cells from primate ovaries were processed by Seurat, with the following criteria: (1) $\log_2$ (the mean expression of the cluster (transcripts per kilobase million [TPM]) was greater than 0.5, (2) the power value was greater than 0.25, (3) the percentage of such cluster cells (PCT.1) was greater than 0.3. Cells were clustered into 8 types according to the previous study,[2] C8 cluster (2.04% [53 of 2,601]) was defined as other cells with no representative markers and are not shown in the t-SNE map. Differentially expressed genes of stromal cells between young and aged ovaries were shown in Table S3.

Enrichment analysis in DisGeNET

DisGeNET (version 4.0) is an online platform with integrated information on human disease, which is used to analyze disease-associated genes.[49] DisGeNET contains 429,036 gene and disease associations and links 17,381 genes to 15,093 diseases, and so on. We analyzed the DEGs of stromal cells between young and old ovaries in DisGeNET to identify the disease enrichment.

Isolation and cell culture

Ovarian stromal cells were isolated according to a previous study.[50] Ovaries were collected from premenopausal women with hysterectomies and salpingectomies for benign indications at the Department of Obstetrics and Gynecology, Tongji Hospital approved by the Ethics Committee of Tongji Hospital (ClinicalTrials.gov identifier NCT01267851). Briefly, freshly collected samples were washed three times in sterilized phosphate-buffered saline (PBS), and then tissues were minced into little fragments and digested with collagenase II (1 mg/mL; Sigma-Aldrich), hyaluronidase (1 mg/mL; Sigma-Aldrich), and DNase I (1 U/mL; Thermo Fisher Scientific) in DMEM (11965084; Gibco) at 37°C for 2 h. Then, they were centrifuged, resuspended with red blood cell lysate for 5 min and centrifuged again. The tissue fragments were resuspended with DMEM supplemented with 10% fetal bovine serum (FBS; 16140071; Gibco), 100 U/mL penicillin, and 100 mg/mL streptomycin (15140-122; Gibco) and transferred to two cell culture flasks. Cells were maintained in DMEM at 37°C with 5% CO_2, supplemented with penicillin-streptomycin and 10% FBS.

Masson staining

In brief, the formaldehyde-fixed and paraffin-embedded (FFPE) sections were deparaffinized and rehydrated, and re-fixed in Bouin's solution. Then, stain in Weigert's iron hematoxylin working solution and Biebrich scarlet-acid fuchsin solution sequentially. And the sections were differentiated in the phosphomolybdic-phosphotungstic acid solution until the collagen is not red. Transfer sections directly to aniline blue solution and stain for 5–10 min. Then, rinse and differentiate in 1% acetic acid solution. Finally, they were dehydrated very quickly through 95% ethyl alcohol, absolute ethyl alcohol, and cleared in xylene.

Cell senescence beta-galactoside enzyme staining

Cell senescence beta-galactoside enzyme staining was performed as previously reported.[51] Initially, fix cells with fixative solution for 10–15 min at room temperature. Then, β-galactosidase staining solution was added to the wells, and the plate was incubated at 37°C at least overnight in a dry incubator. Finally, check the cells under a microscope (200× total magnification) for the development of blue color.

Immunofluorescence

The animal experiments were approved by the Animal Experiment Ethics Committee of Tongji Hospital and performed d under the guidelines of the Laboratory Animal Care Center of Tongji Hospital. Immunofluorescence was performed as described previously.[52] Cells were transferred on glass overnight, formalin-fixed, permeabilized with Triton X-100 (9002-93-1; Sigma-Aldrich), blocked, incubated with target antibody (Table S6), and imaged using Olympus fluorescence microscopy (BX53; Olympus). The average fluorescence intensity was analyzed using ImageJ software.

Immunohistochemistry

The 4 μm FFPE sections were deparaffinized and antigen retrieved. Endogenous peroxidase was inactivated by 3% H_2O_2 to prevent false-positive staining. The non-specific binding proteins were blocked by BSA (5%; Servicebio). The primary antibody was incubated at 4°C overnight, followed by an HRP-linked secondary antibody for 30 min. The slides were then stained with the DAB kit (Servicebio). The score was evaluated via Image-Pro Plus.

Western blot

Cells were collected and washed with PBS and then lysed with RIPA lysis buffer (Beyotime) supplemented with a protease inhibitor cocktail (Roche). Total protein amount was measured, and 30 μg total lysate per sample was subjected to SDS-PAGE followed by immunodetection with primary antibody and the corresponding horseradish peroxidase (HRP)-linked secondary antibody (ab6721; Abcam). Enhanced chemiluminescence (Pierce) was added for imaging with ChemiDoc system. High-kilodalton target band were performed by 10% Precast Protein Plus Gel (36233ES10; Yeasen, Shanghai, China).

Interference of *EGFR* expression

The *EGFR* was interfered by siRNA (5′-GCAAAGUGUGUAACGG AAUAGGUAU-3′; RiboBio Co., Ltd.). Small interfering RNA (siRNA) was transfected using Lipofectamine 3000 (Thermo Fisher Scientific) according to the protocols on the user guide. In brief, cells were seeded to be 70%–90% confluent at transfection. Subsequently, Lipofectamine 3000 was diluted in the Opti-MEM medium (Gibco). The siRNA was mixed with Opti-MEM. Following that, mix the siRNA and Lipofectamine 3000 and incubate for 10–15 min at room temperature. Then, discard the medium in the plate and add the siRNA-lipid complex to the cells. After 72 h of incubation at 37°C, the cells were harvested for the following analysis.

ECM cell adhesion assay

Cell adhesion assay was performed as described previously.[53] Briefly, cells were added into Millicell Hanging Cell Culture Insert (MCRP24H48; Millipore) that were precoated with collagen I, fibronectin, and laminin (Sigma-Aldrich). Plates were incubated for 1 h at 37°C. Then nonadherent cells were removed by gentle washing with PBS. The adhesion cells were fixed and embedded with formaldehyde and paraffin before H&E staining.

RNA-seq and proteomics data of ovaries and correlation analysis

Proteomics data of ovaries were downloaded from the Enhancing GTEx (eGTEx) project of GTEx Portal (https://gtexportal.org/home/). Five human ovaries were sequenced TMT-MS3 based quantitative mass spectrometry (Table S7). RNA-seq data of 180 human ovaries were downloaded from GTEx Portal (https://gtexportal.org/home/). Correlated analysis between AR or ESR1 and target genes were performed by Pearson test. We used a non-log expression value (TPM) for calculation and used the log-scale TPM for visualization.

Pathway and process enrichment analysis

Pathway and process enrichment analysis of DEGs was performed by Metascape.[54] Gene Ontology (GO) and Kyoto Encyclopedia of Genes and Genomes (KEGG) analyses of differentially expressed genes were performed using GOplot, org.Hs.eg.db, and clusterProfiler packages and visualized using the ggplot2 package.

Transcription factors analysis

Transcription factors analysis of DEGs of ovaries between young and aged NHPs were analyzed by the online tool, TRRUST (v2.0) (https://www.grnpedia.org/trrust/). It includes 8,444 transcription factor-target regulatory relationships of 800 human transcription factors.[55] Transcription factor prediction of EGFR, BTG2, and MYC was performed by Toolkit (http://dbtoolkit.cistrome.org/), which contains 47,000 human and mouse samples with about 24,000 datasets.[22] Regulatory potential (RP) was used to estimate the possibility that the transcription factor could regulate the target gene.

ChIP-seq visualization

ChIP-seq data of H3K27ac (NHLF, NHEK, K562, HUVEC, HSMM, H1-hESC, and GM12878), were downloaded and visualized by UCSC Genome Browser (GRCh38/hg38), region of Chr7:55012320-55 224166. ENCODE candidate *cis*-regulatory elements (cCREs) of *EGFR* (chr7:55012320-55224166) combined from all cell types were visualized by UCSC Genome Browser (https://genome-asia.ucsc.edu). ChIP-seq data of AR (GSM696842, GSM1327871, GSM15 86665, GSM1328955, GSM2092844, GSM1358405, GSM1328955, GSM2092844, GSM1716770, GSM2235689, GSM2235686, GSM141 0768, GSM759660, GSM2058879, GSM759659, GSM2086303) and ESR1 (GSM2664041, GSM2257820) were downloaded from Cistrome Data Browser (http://dbtoolkit.cistrome.org/) and were visualized by WashU Browser.

Statistical analysis

Data are presented as mean ± SD. All statistical analyses were performed on the statistical package of GraphPad Prism 9 (version 6.02). Spearman correlation analysis was used to assess the correlation. Two experimental groups were compared by using Student's t test for unpaired data. Where more than two groups were compared, a one-way ANOVA with Bonferroni's correction was used. p values <0.05 were considered to indicate statistical significance. The chi-square test was used when the variable in question was categorical. p values are indicated using asterisks as follows: *$p < 0.05$, **$p < 0.01$, ***$p < 0.001$, and ****$p < 0.0001$.

AVAILABILITY OF DATA AND MATERIALS

Single-cell RNA-seq data were downloaded from GEO: GSE108097 and GSE130664. ChIP-seq data of H3K27ac were downloaded and visualized by UCSC Genome Browser (GRCh38/hg38). ChIP-seq data of AR and ESR1 were downloaded from Cistrome Data Browser. RNA-seq and proteomics data of ovaries were downloaded from the GTEx Portal. Any additional information required to reanalyze the data reported in this paper is available from the lead contact upon request.

SUPPLEMENTAL INFORMATION

Supplemental information can be found online at https://doi.org/10.1016/j.omtn.2022.11.020.

ACKNOWLEDGMENTS

This work was funded by the National Key R&D Program of China (grant 2021YFC2701201), the National Natural Science Foundation of China (grant 82203453), the China Postdoctoral Science Foundation (grant 2021M690259), the Shenzhen Science and Technology Innovation Committee (grants JCYJ20210324105808022 and RCBS20210706092345027), and the Research Foundation of Peking University Shenzhen Hospital (grant JCYJ2020009). We thank all the researchers who uploaded their research data to the public database for their great help in our research. We would like to thank the UCSC Genome Browser and WashU Browser.

AUTHOR CONTRIBUTIONS

C.C., P.W., and H.L. developed the concepts. C.C., Y.W., S.C., R.Y., and P.Z. designed the experiments and performed data analysis. C.H. and D.C. provided feedback. C.C., P.W., H.L., and P.Z. funding acquisition.

DECLARATION OF INTERESTS

The authors declare no competing interests.

REFERENCES

1. Rimon-Dahari, N., Yerushalmi-Heinemann, L., Alyagor, L., and Dekel, N. (2016). Ovarian folliculogenesis. Results Probl. Cell Differ. *58*, 167–190.
2. Wang, S., Zheng, Y., Li, J., Yu, Y., Zhang, W., Song, M., Liu, Z., Min, Z., Hu, H., Jing, Y., et al. (2020). Single-cell transcriptomic atlas of primate ovarian aging. Cell *180*, 585–600.e19.
3. Sánchez, F., and Smitz, J. (2012). Molecular control of oogenesis. Biochim. Biophys. Acta *1822*, 1896–1912.

4. Broekmans, F.J., Soules, M.R., and Fauser, B.C. (2009). Ovarian aging: mechanisms and clinical consequences. Endocr. Rev. *30*, 465–493.
5. Tilly, J.L., and Sinclair, D.A. (2013). Germline energetics, aging, and female infertility. Cell Metab. *17*, 838–850.
6. Perry, J.R.B., Murray, A., Day, F.R., and Ong, K.K. (2015). Molecular insights into the aetiology of female reproductive ageing. Nat. Rev. Endocrinol. *11*, 725–734.
7. Amargant, F., Manuel, S.L., Tu, Q., Parkes, W.S., Rivas, F., Zhou, L.T., Rowley, J.E., Villanueva, C.E., Hornick, J.E., Shekhawat, G.S., et al. (2020). Ovarian stiffness increases with age in the mammalian ovary and depends on collagen and hyaluronan matrices. Aging Cell *19*, e13259.
8. Feng, Y., Cui, P., Lu, X., Hsueh, B., Möller Billig, F., Zarnescu Yanez, L., Tomer, R., Boerboom, D., Carmeliet, P., Deisseroth, K., and Hsueh, A.J.W. (2017). CLARITY reveals dynamics of ovarian follicular architecture and vasculature in three-dimensions. Sci. Rep. *7*, 44810.
9. Briley, S.M., Jasti, S., McCracken, J.M., Hornick, J.E., Fegley, B., Pritchard, M.T., and Duncan, F.E. (2016). Reproductive age-associated fibrosis in the stroma of the mammalian ovary. Reproduction *152*, 245–260.
10. Zhang, Z., Schlamp, F., Huang, L., Clark, H., and Brayboy, L. (2020). Inflammaging is associated with shifted macrophage ontogeny and polarization in the aging mouse ovary. Reproduction *159*, 325–337.
11. Biernacka, A., and Frangogiannis, N.G. (2011). Aging and cardiac fibrosis. Aging Dis. *2*, 158–173.
12. Reeves, G. (1971). Specific stroma in the cortex and medulla of the ovary. Cell types and vascular supply in relation to follicular apparatus and ovulation. Obstet. Gynecol. *37*, 832–844.
13. Kinnear, H.M., Tomaszewski, C.E., Chang, F.L., Moravek, M.B., Xu, M., Padmanabhan, V., and Shikanov, A. (2020). The ovarian stroma as a new frontier. Reproduction *160*, R25–R39.
14. Berkholtz, C.B., Shea, L.D., and Woodruff, T.K. (2006). Extracellular matrix functions in follicle maturation. Semin. Reprod. Med. *24*, 262–269.
15. Tian, Y., Shen, W., Lai, Z., Shi, L., Yang, S., Ding, T., Wang, S., and Luo, A. (2015). Isolation and identification of ovarian theca-interstitial cells and granulose cells of immature female mice. Cell Biol. Int. *39*, 584–590.
16. Konishi, I., Fujii, S., Okamura, H., Parmley, T., and Mori, T. (1986). Development of interstitial cells and ovigerous cords in the human fetal ovary: an ultrastructural study. J. Anat. *148*, 121–135.
17. Gu, X., Li, S.Y., and DeFalco, T. (2022). Immune and vascular contributions to organogenesis of the testis and ovary. FEBS J. *289*, 2386–2408.
18. Lu, H., Ma, L., Zhang, Y., Feng, Y., Zhang, J., and Wang, S. (2022). Current animal model systems for ovarian aging research. Aging Dis. *13*, 1183–1195.
19. Zhang, Y., Yan, Z., Qin, Q., Nisenblat, V., Chang, H.M., Yu, Y., Wang, T., Lu, C., Yang, M., Yang, S., et al. (2018). Transcriptome landscape of human folliculogenesis reveals oocyte and granulosa cell interactions. Mol. Cell *72*, 1021–1034.e4.
20. Han, X., Wang, R., Zhou, Y., Fei, L., Sun, H., Lai, S., Saadatpour, A., Zhou, Z., Chen, H., Ye, F., et al. (2018). Mapping the mouse cell atlas by microwell-seq. Cell *173*, 1307.
21. Firestone, G.L., and Sundar, S.N. (2009). Minireview: modulation of hormone receptor signaling by dietary anticancer indoles. Mol. Endocrinol. *23*, 1940–1947.
22. Zheng, R., Wan, C., Mei, S., Qin, Q., Wu, Q., Sun, H., Chen, C.H., Brown, M., Zhang, X., Meyer, C.A., and Liu, X.S. (2019). Cistrome Data Browser: expanded datasets and new tools for gene regulatory analysis. Nucleic Acids Res. *47*, D729–D735.
23. Rivera, A.D., Pieropan, F., Chacon-De-La-Rocha, I., Lecca, D., Abbracchio, M.P., Azim, K., and Butt, A.M. (2021). Functional genomic analyses highlight a shift in Gpr17-regulated cellular processes in oligodendrocyte progenitor cells and underlying myelin dysregulation in the aged mouse cerebrum. Aging Cell *20*, e13335.
24. Rivera, A.D., Pieropan, F., Williams, G., Calzolari, F., Butt, A.M., and Azim, K. (2022). Drug connectivity mapping and functional analysis reveal therapeutic small molecules that differentially modulate myelination. Biomed. Pharmacother. *145*, 112436.
25. Chava, S., Bugide, S., Zhang, X., Gupta, R., and Wajapeyee, N. (2022). Betacellulin promotes tumor development and EGFR mutant lung cancer growth by stimulating the EGFR pathway and suppressing apoptosis. iScience *25*, 104211.
26. Walker, M.L., Anderson, D.C., Herndon, J.G., and Walker, L.C. (2009). Ovarian aging in squirrel monkeys (Saimiri sciureus). Reproduction *138*, 793–799.
27. Li, C.J., Lin, L.T., Tsai, H.W., Chern, C.U., Wen, Z.H., Wang, P.H., and Tsui, K.H. (2021). The molecular regulation in the pathophysiology in ovarian aging. Aging Dis. *12*, 934–949.
28. Fan, X., Bialecka, M., Moustakas, I., Lam, E., Torrens-Juaneda, V., Borggreven, N.V., Trouw, L., Louwe, L.A., Pilgram, G.S.K., Mei, H., et al. (2019). Single-cell reconstruction of follicular remodeling in the human adult ovary. Nat. Commun. *10*, 3164.
29. Achterberg, V.F., Buscemi, L., Diekmann, H., Smith-Clerc, J., Schwengler, H., Meister, J.J., Wenck, H., Gallinat, S., and Hinz, B. (2014). The nano-scale mechanical properties of the extracellular matrix regulate dermal fibroblast function. J. Invest. Dermatol. *134*, 1862–1872.
30. Nautiyal, J., Du, J., Yu, Y., Kanwar, S.S., Levi, E., and Majumdar, A.P.N. (2012). EGFR regulation of colon cancer stem-like cells during aging and in response to the colonic carcinogen dimethylhydrazine. Am. J. Physiol. Gastrointest. Liver Physiol. *302*, G655–G663.
31. Malecka-Panas, E., Kordek, R., Biernat, W., Tureaud, J., Liberski, P.P., and Majumdar, A.P. (1997). Differential activation of total and EGF receptor (EGF-R) tyrosine kinase (tyr-k) in the rectal mucosa in patients with adenomatous polyps, ulcerative colitis and colon cancer. Hepatogastroenterology *44*, 435–440.
32. Schmelz, E.M., Levi, E., Du, J., Xu, H., and Majumdar, A.P.N. (2004). Age-related loss of EGF-receptor related protein (ERRP) in the aging colon is a potential risk factor for colon cancer. Mech. Ageing Dev. *125*, 917–922.
33. Siddiqui, S., Fang, M., Ni, B., Lu, D., Martin, B., and Maudsley, S. (2012). Central role of the EGF receptor in neurometabolic aging. Int. J. Endocrinol. *2012*, 739428.
34. Xu, X., Liu, Q., Zhang, C., Ren, S., Xu, L., Zhao, Z., Dou, H., Li, P., Zhang, X., Gong, Y., and Shao, C. (2019). Inhibition of DYRK1A-EGFR axis by p53-MDM2 cascade mediates the induction of cellular senescence. Cell Death Dis. *10*, 282.
35. Shang, D., Sun, D., Shi, C., Xu, J., Shen, M., Hu, X., Liu, H., and Tu, Z. (2020). Activation of epidermal growth factor receptor signaling mediates cellular senescence induced by certain pro-inflammatory cytokines. Aging Cell *19*, e13145.
36. Liu, G., Xie, Y., Su, J., Qin, H., Wu, H., Li, K., Yu, B., and Zhang, X. (2019). The role of EGFR signaling in age-related osteoporosis in mouse cortical bone. FASEB J. *33*, 11137–11147.
37. Kenngott, R.A.M., Scholz, W., and Sinowatz, F. (2016). Ultrastructural aspects of the prenatal bovine ovary differentiation with a special focus on the interstitial cells. Anat. Histol. Embryol. *45*, 357–366.
38. Abd-Elkareem, M. (2017). Cell-specific immuno-localization of progesterone receptor alpha in the rabbit ovary during pregnancy and after parturition. Anim. Reprod. Sci. *180*, 100–120.
39. Juengel, J.L., Heath, D.A., Quirke, L.D., and McNatty, K.P. (2006). Oestrogen receptor alpha and beta, androgen receptor and progesterone receptor mRNA and protein localisation within the developing ovary and in small growing follicles of sheep. Reproduction *131*, 81–92.
40. Escoffery, C.T., Blake, G.O., and Sargeant, L.A. (2002). Histopathological findings in women with postmenopausal bleeding in Jamaica. West Indian Med. J. *51*, 232–235.
41. Matt, D.W., Kauma, S.W., Pincus, S.M., Veldhuis, J.D., and Evans, W.S. (1998). Characteristics of luteinizing hormone secretion in younger versus older premenopausal women. Am. J. Obstet. Gynecol. *178*, 504–510.
42. Thompson, M.A., and Adelson, M.D. (1993). Aging and development of ovarian epithelial carcinoma: the relevance of changes in ovarian stromal androgen production. Adv. Exp. Med. Biol. *330*, 155–165.
43. Adashi, E.Y. (1994). The climacteric ovary as a functional gonadotropin-driven androgen-producing gland. Fertil. Steril. *62*, 20–27.
44. Cheng, Y., Ma, Z., Kim, B.H., Wu, W., Cayting, P., Boyle, A.P., Sundaram, V., Xing, X., Dogan, N., Li, J., et al. (2014). Principles of regulatory information conservation between mouse and human. Nature *515*, 371–375.
45. Dowell, R.D. (2011). The similarity of gene expression between human and mouse tissues. Genome Biol. *12*, 101.
46. Cardoso-Moreira, M., Sarropoulos, I., Velten, B., Mort, M., Cooper, D.N., Huber, W., and Kaessmann, H. (2020). Developmental gene expression differences between humans and mammalian models. Cell Rep. *33*, 108308.

47. Teufel, A., Itzel, T., Erhart, W., Brosch, M., Wang, X.Y., Kim, Y.O., von Schönfels, W., Herrmann, A., Brückner, S., Stickel, F., et al. (2016). Comparison of gene expression patterns between mouse models of nonalcoholic fatty liver disease and liver tissues from patients. Gastroenterology *151*, 513–525.e0.

48. Madissoon, E., Töhönen, V., Vesterlund, L., Katayama, S., Unneberg, P., Inzunza, J., Hovatta, O., and Kere, J. (2014). Differences in gene expression between mouse and human for dynamically regulated genes in early embryo. PLoS One *9*, e102949.

49. Piñero, J., Bravo, À., Queralt-Rosinach, N., Gutiérrez-Sacristán, A., Deu-Pons, J., Centeno, E., García-García, J., Sanz, F., and Furlong, L.I. (2017). DisGeNET: a comprehensive platform integrating information on human disease-associated genes and variants. Nucleic Acids Res. *45*, D833–D839.

50. Cui, L., Bao, H., Liu, Z., Man, X., Liu, H., Hou, Y., Luo, Q., Wang, S., Fu, Q., and Zhang, H. (2020). hUMSCs regulate the differentiation of ovarian stromal cells via TGF-beta1/Smad3 signaling pathway to inhibit ovarian fibrosis to repair ovarian function in POI rats. Stem Cell Res. Ther. *11*, 386.

51. Baker, D.J., Jeganathan, K.B., Cameron, J.D., Thompson, M., Juneja, S., Kopecka, A., Kumar, R., Jenkins, R.B., de Groen, P.C., Roche, P., and van Deursen, J.M. (2004). BubR1 insufficiency causes early onset of aging-associated phenotypes and infertility in mice. Nat. Genet. *36*, 744–749.

52. Cao, C.H., Liu, R., Lin, X.R., Luo, J.Q., Cao, L.J., Zhang, Q.J., Lin, S.R., Geng, L., Sun, Z.Y., Ye, S.K., et al. (2021). LRP1B mutation is associated with tumor HPV status and promotes poor disease outcomes with a higher mutation count in HPV-related cervical carcinoma and head & neck squamous cell carcinoma. Int. J. Biol. Sci. *17*, 1744–1756.

53. Hosseini, F., Hassannia, H., Mahdian-Shakib, A., Jadidi-Niaragh, F., Enderami, S.E., Fattahi, M., Anissian, A., Mirshafiey, A., and Kokhaei, P. (2017). Targeting of cross-talk between tumor and tumor microenvironment by beta-D mannuronic acid (M2000) in murine breast cancer model. Cancer Med. *6*, 640–650.

54. Zhou, Y., Zhou, B., Pache, L., Chang, M., Khodabakhshi, A.H., Tanaseichuk, O., Benner, C., and Chanda, S.K. (2019). Metascape provides a biologist-oriented resource for the analysis of systems-level datasets. Nat. Commun. *10*, 1523.

55. Han, H., Cho, J.W., Lee, S., Yun, A., Kim, H., Bae, D., Yang, S., Kim, C.Y., Lee, M., Kim, E., et al. (2018). TRRUST v2: an expanded reference database of human and mouse transcriptional regulatory interactions. Nucleic Acids Res. *46*, D380–D386.